Defect energetics in aluminium

1991 J. Phys.: Condens. Matter 3 8777

(http://iopscience.iop.org/0953-8984/3/45/003)

J. Phys.: Condens. Matter 3 (1991) 8777–8792. Printed in the UK

Defect energetics in aluminium

P J H Denteneer† and J M Soler‡

† Instituut-Lorentz, University of Leiden, PO Box 9506, 2300 RA Leiden, The Netherlands

‡ Departamento de Física de la Materia Condensada (C-III), Universidad Autónoma de Madrid, E-28049 Madrid, Spain

Received 3 May 1991, in final form 2 September 1991

Abstract. Formation energies of the vacancy and self-interstitial in Al, as well as energies of intrinsic, extrinsic and twin-boundary stacking faults are calculated from first principles. The electronic structure and forces on the atoms are calculated in the framework of the augmented plane wave method using the algorithm proposed by Williams and Soler.

1. Introduction

The study of defects in solids is both an intellectual challenge, because the reduced symmetry of the problem complicates the analysis, and of technological relevance, because some defects may already be present in thermal equilibrium, whereas others are easily introduced in the growth or processing (e.g. heating, ion implantation) of crystals. Therefore defects are intrinsic to real crystals and determine or modify the properties of real materials. For instance, the presence of shallow impurities in semiconductors causes the conducting properties of semiconductors and their control is the basis of the modern electronics industry. Also, the creation and behaviour of vacancies and interstitials rule the mechanism of void formation in pure metals, which is one of the prime examples of irradiation damage in metals. Void formation in turn causes undesirable embrittlement and/or swelling of, for instance, nuclear reactor materials.

Defects may be classified according to the number of dimensions in which they are spatially restricted. One may distinguish between point defects, like vacancies, interstitials, and impurities, which are bounded in three dimensions, line defects, like dislocations, which are bounded in two dimensions, and planar defects, like stacking faults and grain boundaries, which are restricted only in one dimension.

Progress has been made in recent years in calculating the macroscopic properties of real materials from the quantum mechanical behaviour on the microscopic level of atoms and electrons [1,2]. This development will lead to a quantum mechanical understanding of the mechanical behaviour of solids through atomistic models of deformation, fracture and crack propagation. Such atomistic models will not necessarily make use of first-principles descriptions of all (also mutual) interactions between atoms and electrons. It is more likely that such models will include so called *empirical potentials* to effectively describe interatomic interactions [2]. Employing empirical interatomic potentials greatly reduces the computational task compared to a

0953-8984/91/458777+16$03.50

first-principles description, hence the preference for empirical potentials in treating complicated models of, for instance, grain boundaries and dislocations. However, there will still be a need for first-principles calculations of defect properties. For less complicated defects, like vacancies, first-principles calculations provide a way to scrutinize the reliability of results obtained using empirical potentials.

Essential for a quantum mechanical description of defective crystals is the ability to accurately compute the forces that the atoms experience. In calculations for semiconductors Hellmann–Feynman forces [3] are routinely obtained by methods using pseudopotentials and plane wave expansions of the electronic wavefunctions. In this way, accurate phonon frequencies and optimized defect geometries have been obtained [4,5]. A further development, shown to be feasible by Car and Parrinello [6] is the combination of *ab initio* electronic structure calculations, as mentioned above, and the technique of molecular dynamics. In this approach, the forces on the atoms calculated from quantum mechanics are used as input for the classical equations of motion for the atoms. In contrast to the situation for semiconductors, until recently there were no formulae available to compute atomic forces in solids which are less suited to be treated with pseudopotentials. Soler and Williams have filled this void in a recent paper [7] by providing formulae to compute atomic forces in the framework of the augmented plane wave (APW) method (using the local-density approximation (LDA) to describe exchange and correlation interactions between electrons [1,8]. Moreover, these formulae were implemented in a computer program that solves the Schrödinger equation self-consistently by non-linear optimization by means of a (fictitious) first-order equation of motion [9].

In the present work, we use the methods and computer codes by Soler and Williams to calculate from first principles formation and migration energies of a wide variety of defects in the simple metal aluminium. The rest of the paper is organized as follows: in section 2, we briefly discuss the calculational techniques that are used. We also present results of test calculations for lattice constant, bulk modulus, and phonon frequencies in bulk Al, which establish the reliability of the method for Al. In section 3, calculations and results for planar defects are discussed. We obtain the energies of intrinsic and extrinsic stacking faults and of the twin boundary in good agreement with experiments and, more importantly, with higher accuracy than in the experiments. In section 4, we examine the long-standing problem of the formation energy of the vacancy using our versatile approach. Other properties of the vacancy defect are calculated as well. We furthermore present one of the first studies of another simple point defect: the self-interstitial. Our treatment of the vacancy and self-interstitial has the advantage over other recent studies [10,11] that we include relaxation of the atoms around the point defects and that we do not make use of pseudopotentials. In the previous studies, the formation energy of the vacancy was shown to depend rather heavily on the choice of pseudopotential. Concluding and summarizing remarks are found in section 5.

2. Calculational methods and test calculations

In order to self-consistently solve the Schrödinger equation for the electrons in a periodic arrangement of atoms, Car and Parrinello [6] have proposed to treat the variational parameters (the coefficients in the expansion of the wavefunctions in plane waves) as fictitious dynamical variables. Self-consistency (and total-energy minimization) is then achieved by simulated annealing or by steepest-descent-like methods.

In this way, the computation time increases only as $N \log N$ with the number of plane waves N, as opposed to N^2 or N^3 in conventional methods requiring matrix diagonalizations. This approach furthermore allows for the simultaneous optimization of the atomic geometry by using the quantum mechanical forces on the atoms to do molecular dynamics. In the method used in the present paper, which will be described more extensively elsewhere [12] the approach of Car and Parrinello is carried through in the framework of the APW method. As proposed in [9] a first-order equation of motion is used to govern the time development of the plane wave coefficients C_G:

$$C_G(t+\Delta t) = C_G(t) + \left(\frac{1-\exp[-(H_{GG}-\epsilon)\Delta t]}{H_{GG}-\epsilon}\right) \times \sum_{G'}(H_{GG'}-\epsilon\delta_{GG'})C_{G'}(t) \tag{1}$$

where $H_{GG'}$ are matrix elements of the Hamiltonian and ϵ one-electron energies.

In the APW method, space is divided into two regions: interstitial space, in which the wavefunctions are expanded in plane waves, and non-overlapping spheres centred on every atom, in which the wave function is a linear combination of spherical functions which are matched to the plane waves on the surfaces of the spheres ('augmentation'). Notice that one-electron wavefunctions, rather than individual plane waves, are augmented in this formulation of the APW method. Furthermore, there is no need to construct a secular matrix during the optimization run and therefore no common basis set for all wavefunctions is needed. As a result, the linear approximation [8] for the wavefunctions inside the muffin-tin spheres does not have to be made. The initial wavefunctions are constructed by diagonalizing a muffin-tin Hamiltonian using a minimal LCAO basis set, consisting of atomic orbitals fitted to a single Gaussian.

In the present stage of the computer code, we do not allow the atoms to move during an optimization run yet. So we do not yet perform a simultaneous molecular dynamics simulation. We do however obtain the forces on the atoms [7] in a particular atomic configuration so that in a follow up run the atoms may be moved in the direction of the forces. In this way, the lowest-energy configuration can be found. The present stage of the code can be thought of as the 'APW-equivalent' of the method used by Payne *et al* [13] with pseudopotentials and plane waves. Our relatively new method has been succesfully applied in the first-principles calculation of phonon frequencies in Si and Cu and of the geometry of the N_2 and H_2O molecules [14]. To further test the code we performed an optimization of the hydrogen–phosphorus complex in crystalline silicon and compared with recent pseudopotential calculations [5]; we obtain good agreement for the calculated forces and found the same configuration for the complex to be lowest in energy [15]. We also verified, both for the phonon frequencies in Si and the (H,P) complex in Si, that a substantially smaller number of plane waves suffices in the APW calculations compared wtth the pseudopotential calculations, which use plane waves to describe the wavefunctions everywhere. A short account of the present work on aluminium was given in [16].

In the remainder of this section, we discuss test calculations for bulk Al that were performed to establish parameters to be used in the defect calculations. The three most important parameters determining the accuracy of calculations in the present method are: R_{MT}, the radius of the (muffin-tin) sphere around each atom, E_{PW}, the largest kinetic energy of plane waves included in the expansion of the wavefunction,

and N_{sp}, the number of special points in the irreducible wedge of the first Brillouin zone used to integrate over the Brillouin zone (BZ). R_{MT} may be chosen differently for different types of atoms, but in such a way that no spheres overlap. Special points are obtained using the general Monkhorst–Pack (MP) scheme [17] and integrations over the BZ are performed using the Gaussian-smearing method of Fu and Ho [18], especially suited to treat metallic systems. It is obvious that the choice of R_{MT} and E_{PW} are related; the larger R_{MT}, the smaller the interstitial region, and the fewer plane waves are needed to accurately describe the wavefunction in that region.

Table 1. Total energy of bulk Al as a function of the number of plane waves per atom, N_{PW}, in the basis set. E_{PW} is the kinetic energy above which plane waves are excluded from the basis set. The approximate relation between N_{PW} and E_{PW} is $N_{PW} = \Omega_0 E_{PW}^{3/2}/6\pi^2$, where Ω_0 is the volume per atom. All calculations are for $a_c = 7.6$ au, $R_{MT} = 2.4$ au, and using 28 special k points (see text).

E_{PW} (Ryd)	N_{PW}	E_{tot} (Ryd/atom)
6	27	−482.93141
8	42	−482.93112
10	59	−482.93448
12	77	−482.93170
14	97	−482.93130

We have established that for $R_{MT} = 2.4$ au bulk Al (FCC structure; one atom per primitive unit cell) is already accurately described using $E_{PW} = 6$ Ryd, corresponding to about 27 plane waves per atom. In table 1, the total energy of bulk Al as a function of E_{PW} is given for a lattice constant a_c of 7.6 au, close to the experimental lattice constant. A MP special-point set with $q = 6$, corresponding to 28 k points in the irreducible part of the BZ, is used. The value for $E_{PW} = 10$ Ryd is somewhat anomalous, a fact for which we offer no explanation. In table 2, the total energy and Fermi level for Al are given as a function of N_{sp}, the number of k points in the irreducible part of the BZ, for successively finer MP meshes in the BZ. These calculations are for $a_c = 7.6$ au and with $E_{PW} = 6$ Ryd. We argue that for $q = 6$, E_{tot} and E_F are calculated with sufficient accuracy. Even more so because we will be mainly interested in energy *differences* rather than absolute energies. Of course the choice of the number of k points depends on the required accuracy and will be studied for each of the applications separately below. With $q = 6$ and $E_{PW} = 6$ Ryd, we calculate an equilibrium lattice constant a_{eq} of 7.56 au and a bulk modulus B_0 of 0.87 Mbar [19]. The experimental numbers are: $a_{eq} = 7.62$ au and for B_0 values from 0.72 to 0.88 Mbar are reported [20]. Increasing E_{PW} to 8 Ryd (equivalent to 42 plane waves per atom) only changes a_{eq} to 7.54 au and B_0 to 0.84 Mbar.

We also performed a conventional pseudopotential plane waves calculation using a norm-conserving pseudopotential [21] for Al for comparison. The results are: $a_{eq} = 7.43$ au and $B_0 = 0.86$ Mbar, in agreement with the APW results. In anticipation of our aim to perform calculations for the self-interstitial point defect in Al, we also investigate the case that we have to choose R_{MT} as small as 1.89 au (the distance of a self-interstitial to a host atom is at most 3.8 au, for an interstitial in an octahedral interstitial site). For that case, we have to choose E_{PW} as large as 12 Ryd. To establish this value, we calculate the formation energy at constant volume of a self-interstitial at the octahedral interstitial site $E_{f,v}^{int}$ as a function of E_{PW}. The definition

Table 2. Total energy and Fermi energy of bulk Al as a function of the number of special k points, N_{sp}, used to perform Brillouin zone integrations. The parameter q (see [17]) determines the number of intervals into which the basis vectors of the reciprocal lattice are subdivided to form a mesh in reciprocal space. N_{sp} is determined by q by $N_{sp} = q(q+1)(q+2)/12$. All calculations are for $a_c = 7.6$ au, $R_{MT} = 2.4$ au, and $E_{PW} = 6$ Ryd (see text).

q	N_{sp}	E_{tot} (Ryd/atom)	E_F (Ryd)
2	2	−482.915 18	0.632
4	10	−482.927 84	0.691
6	28	−482.931 41	0.677
8	60	−482.932 10	0.681
10	110	−482.931 72	0.685
12	182	−482.931 58	0.684
16	408	−482.931 51	0.682

of this formation energy will be given in section 4, but for our present purpose it does not matter. The calculation is performed using supercells containing 16 (without interstitial) and 17 (with interstitial) atoms, $a_c = 7.6$ au, and 8 k points in the full BZ of the supercell. Although the number of k points is not sufficient for a reliable quantitative estimate of $E_{f,v}^{int}$ (see section 4) it is sufficient for the present purpose of finding an adequate value for E_{PW} to be used together with the choice $R_{MT} = 1.89$ au. The results are given in table 3. Choosing $E_{PW} = 12$ Ryd (77 plane waves per atom) as a reasonable value to be used in conjunction with $R_{MT} = 1.89$ au, we find $a_{eq} = 7.54$ au and $B_0 = 0.83$ Mbar. Therefore, calculations for the interstitial will be much more computing intensive than for the vacancy, for which $R_{MT} = 2.4$ au and 6 Ryd may be used. Our results using various parameter combinations and methods are compiled in table 4 and compared with previous theoretical calculations [22, 23] and experimental values.

Table 3. Formation energy at constant volume of the self-interstitial defect in Al, $E_{f,v}^{int}$, as a function of kinetic energy cut-off E_{PW} (see text). $E_{f,v}^{int}$ is calculated in a 16-atom supercell as $E_{tot}(17) - (17/16)E_{tot}(16)$ (see also section 4). The calculations are for $a_c = 7.6$ au, $R_{MT} = 1.89$ au, and 8 k points in the full Brillouin zone of the supercell.

E_{PW} (Ryd)	$E_{f,v}^{int}$ (eV)
6	−0.48
8	1.06
10	1.16
12	1.02
14	1.04

From the calculated forces on the atoms in a doubled unit cell in which the atoms are frozen in with displacements corresponding to phonons at zone boundary X, the frequencies of the longitudinal L(X) and transversal T(X) phonons can be calculated [4]. Using $E_{PW} = 6$ Ryd, $R_{MT} = 2.4$ au, and 45 (75) k points for L(X) (T(X)) (equivalent to $q = 10$ for bulk Al; see table 2) we find phonon frequencies of $\nu_{L(X)} = 9.93$ THz and $\nu_{T(X)} = 5.67$ THz. These results are in good agreement with the experimental numbers: $\nu_{L(X)} = 9.68$ THz and $\nu_{T(X)} = 5.81$ THz. In table 5, we give results of calculations using larger E_{PW} (but smaller numbers of k points; 12

Table 4. Calculated ground-state properties of Al (lattice constant a_{eq} and bulk modulus B_0) using various methods and choices of parameters, compared with experimental results.

	a_{eq} (au)	B_0 (Mbar)
Moruzzi *et al* ; KKR [22]	7.60	0.80
Present work; APW, $E_{PW} = 6$ Ryd, $R_{MT} = 2.4$ au	7.56	0.87
Present work; APW, $E_{PW} = 8$ Ryd, $R_{MT} = 2.4$ au	7.53	0.84
Present work; APW, $E_{PW} = 12$ Ryd, $R_{MT} = 1.89$ au	7.55	0.83
Lam and Cohen; norm-conserving pseudopotential [23]	7.58	0.72
Present work; norm-conserving pseudopotential	7.43	0.86
Experiment	7.62	0.72–0.88

for L(X) and 18 for T(X), equivalent to $q = 6$ for bulk Al). Although the calculated frequencies are somewhat sensitive to the number of plane waves and the number of k points, we argue that the forces are calculated with sufficient accuracy to find the equilibrium configuration of a set of atoms. For completeness we note that if we calculate $\nu_{L(X)}$ using norm-conserving pseudopotentials (with $E_{PW} = 24$ Ryd and 45 k points [19]) we find 9.52 THz, in reasonable agreement with the APW results, again confirming their reliability.

Table 5. Calculated longitudinal and transversal phonon frequencies at the zone boundary point X of the BZ of Al, $\nu_{L(X)}$ and $\nu_{T(X)}$, respectively, as a function of kinetic energy cut-off E_{PW} (see text). The experimental results are taken from [23]. The calculations are for $a_c = 7.6$ au, $R_{MT} = 2.4$ au, and using 12 (L(X)) and 18 (T(X)) special k points in the irreducible part of the Brillouin zone of the (doubled) unit cell in which the phonon modes are frozen in.

E_{PW} (Ryd)	$\nu_{L(X)}$ (THz)	$\nu_{T(X)}$ (THz)
6	10.46	5.59
8	10.19	5.48
10	10.04	5.46
12	9.91	5.43
14	9.87	5.42
Experiment	9.68	5.81

We conclude that with the present method energies and forces in bulk Al can be computed with sufficient accuracy using modest numbers of plane waves and k points.

3. Planar defects in aluminium

Although the energies of stacking faults are in general very small (5–100 meV per unit cell of a fault layer), one of us has shown earlier that they can be accurately calculated from first principles [24]. In this approach, stacking faults along the [111] direction are seen as the limiting structures of a series of polytypes. Polytypes are periodically repeated stacking sequences of atomic layers, in which all atoms have the same coordination as in the basic, unfaulted structure. With this point of view,

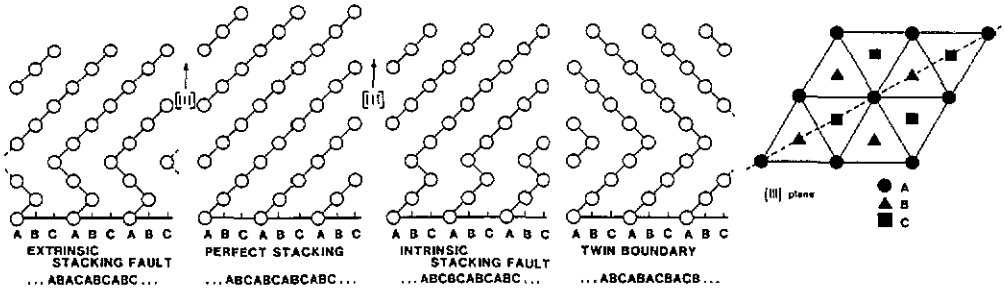

Figure 1. Stacking faults along the [111] direction for FCC metals. In each (111) plane the atoms are arranged in equilateral triangles. If in one plane the atoms occupy positions A, in the next plane of atoms along [111] they can either occupy positions B or C and still be all six-fold coordinated. In a perfect FCC crystal structure the stacking sequence is ABCABC...; the intrinsic and extrinsic stacking faults and twin-boundary have stacking sequences ABACABC..., ABCBCABC..., and ABCABACBACB..., respectively.

a systematic parametrization of the energies of polytypes in terms of interaction constants between layers allows for the calculation of stacking-fault energies.

Smith *et al* have pointed out similarities between the ANNNI model and the occurrence of polytypes [25]. Therefore it is conceivable that the energies of polytypes may be parametrized using:

$$E = E_0 - J_1 \sum_i S_i S_{i+1} - J_2 \sum_i S_i S_{i+2} - J_3 \sum_i S_i S_{i+3} - \cdots \qquad (2)$$

where the summation is over layers. The connection with Ising spins is that a layer has $S_i = +1$ or -1 depending on whether or not the layer is surrounded by layers as in the ideal, unfaulted, stacking sequence. The parameters J_n $(n = 0, 1, 2, \ldots)$ are interaction energies between two layers a distance nd apart, where d is the layer thickness. E_0 is the energy contribution, common to all polytypes, which results if all interactions between layers are disregarded. Total energies of all polytypes are easily expressed in the parameters E_0 and J_n (n = 0,1,2,...) [24]. For semiconductors we have found that usually total energies (calculated from first principles) for three simple (possibly fictitious) polytypes suffice to extract stacking-fault energies in very good agreement with available experiments. The same approach is easily applied to stacking faults along [111] in FCC metals. Blandin *et al* have used similar reasoning before to calculate stacking-fault energies in metals using the nearly-free-electron approximation [26].

The unfaulted FCC structure of Al can be represented by a repeated stacking sequence along [111] of three atomic layers: ABCABC.... The intrinsic stacking fault (ISF) is obtained by removing one atomic layer from the perfect sequence: ABCBCABCABC..., the extrinsic stacking fault (ESF) by inserting one atomic layer: ABACABCABC..., and the [111] 60° [111] grain boundary or twin boundary (TWB) by reversing the stacking order at a certain point: ...ABCABACB... (see figure 1). In [24], it is shown how the energy per unit cell in a layer for the ISF and ESF may be expressed in the interaction energies J_n. Using the stacking sequence given above a similar result is easily obtained for the TWB. Here, we only give the results:

$$\begin{aligned} E_{\mathrm{ISF}} &= 4J_1 + 4J_2 + 4J_3 + \ldots \\ E_{\mathrm{ESF}} &= 4J_1 + 8J_2 + 8J_3 + \ldots \\ E_{\mathrm{TWB}} &= 2J_1 + 4J_2 + 6J_3 + \ldots \end{aligned} \tag{3}$$

From (3) it is clear that if one assumes that the J_n with $n = 2, 3, \ldots$ may be neglected compared to J_1, one recovers the well known rule of thumb for stacking-fault energies: $E_{\mathrm{ISF}} = E_{\mathrm{ESF}} = 2E_{\mathrm{TWB}}$ [27]. This rule is apparently based upon the fact that the ISF and ESF contain two layers that are hexagonally packed (all other layers, like in the perfect structure, are cubically packed) and the TWB has only one layer that is hexagonally packed. If one also retains J_2, we obtain a distinction between the ISF and ESF, such that depending on the sign of J_2, either the ISF ($J_2 < 0$) or the ESF ($J_2 > 0$) has a higher formation energy. For Si, diamond [24], and Al (see below), we find $J_2 < 0$, but this does not always have to be the case. The relation $E_{\mathrm{ESF}} = 2E_{\mathrm{TWB}}$ is only violated if J_3 cannot be neglected.

Here we retain J_1 and J_2 to be able to discriminate between all three stacking faults. In that case, J_1 and J_2 can be calculated from the differences in total energy between the three polytypes with repeat units ABC (FCC Al, polytype 3C), AB (HCP Al, polytype 2H), and ABCB (polytype 4H), having 3, 2 and 4 atoms per (hexagonal) unit cell, respectively. The total energies for the three polytypes of Al are calculated with the parameters $E_{\mathrm{PW}} = 6$ Ryd and $R_{\mathrm{MT}} = 2.4$ au and an increasingly dense sampling of the respective BZ. To improve convergence of total-energy differences with increasing numbers of k points we select k point sets containing exactly the same k points for each of the three polytypes [28]. For this procedure it is essential to describe the polytype 3C in an hexagonal unit cell with 3 atoms, instead of the primitive, cubic, unit cell with 1 atom. Furthermore, one needs the generalization of the Monkhorst–Pack scheme for special k points given by MacDonald [29]. Moreover, we need a large number of k points since all three polytypes are metals and we need to calculate a reasonably accurate Fermi level. The results of these calculations are given in table 6. In our most accurate calculation, we use 240, 292 and 120 k points in the irreducible parts of the BZ for 2H, 3C and 4H, respectively. These numbers correspond to a sampling of reciprocal space a factor of about 30 more dense than used in the bulk calculations of the previous section. We find that for large enough k point sets the Fermi energy (with respect to the average interstitial potential) is approximately equal for all three polytypes.

For the energy difference between 2H and 3C, which equals $2J_1$ [24], we then find: 31.5 meV/atom. For the energy difference between 2H and 4H, which equals $J_1 - 2J_2$, we find: 19.7 meV/atom. The 3C polytype is lowest and the 2H polytype highest in energy of these three. From calculations with smaller numbers of k points we estimate the error bar on these energy differences to be about 1 meV/atom. The fact that $J_1 = 15.7$ meV and $J_2 = -2.0$ meV suggests a posteriori that neglecting higher order interaction constants is a reasonable approximation. The signs and ratio of J_1 and J_2 are similar to those found for polytypes of silicon and carbon [24].

The stacking-fault energies γ_{ISF}, γ_{ESF}, and γ_{TWB} most often considered in the literature are obtained by dividing the energies of (3) by $\frac{1}{4}a_c^2\sqrt{3}$, the area of a hexagon defining a unit cell in one layer, with a_c the lattice constant of the corresponding FCC structure. For consistency the nearest-neighbour (NN) distances in all three polytypes have to be chosen equal to the NN distance in bulk Al (= 5.4 au). Consequently, our calculated stacking fault energies do not include atomic relaxations

Table 6. Total energies of polytypes 3C, 2H, and 4H of Al as a function of Brillouin-zone sampling. Energies E are in Ryd/atom and energy differences δ_1 (between 2H and 3C) and δ_h (between 2H and 4H) are in meV/atom. The parameter q_{2H} determines the number of intervals into which the basis vectors of the reciprocal lattice of the polytype 2H are subdivided to form a mesh in reciprocal space. For these calculations, all polytypes are described in an hexagonal unit cell; the third component of q_{2H} determines the number of intervals along the hexagonal axis. If $q_{2H} = (q_a, q_a, q_c)$, then the corresponding $q_{3C} = (q_a, q_a, \frac{2}{3}q_c)$ and $q_{4H} = (q_a, q_a, \frac{1}{2}q_c)$. For 4H, a vector $[0,0,1/q_c]$ (coordinates with respect to reciprocal basis for 4H) is added to each k point if $q_c/2$ is odd to obtain exactly the same k points in all three cases (see text). If $\frac{2}{3}q_c$ is not an integer no such equivalent k point set exists for 3C.

q_{2H}	E(3C)	δ_1	E(2H)	δ_h	E(4H)
(7,7,4)	—	—	−482.93026	35.0	−482.93283
(9,9,6)	−482.93010	30.1	−482.92789	20.6	−482.92940
(11,11,8)	—	—	−482.92951	22.1	−482.93113
(15,15,10)	—	—	−482.92928	20.9	−482.93082
(19,19,12)	−482.93142	31.5	−482.92910	19.7	−482.93055

near the fault. Such relaxations are believed to lower the calculated energies only by a few per cent. Using our calculated energy differences, we have: $\gamma_{ISF} = 126 \pm 12$ mJ m^{-2}, $\gamma_{ESF} = 108 \pm 11$ mJ m^{-2}, and $\gamma_{TWB} = 54 \pm 6$ mJ m^{-2}, where we have indicated estimated error bars. The value of γ_{ISF} is in excellent agreement with the experimental result of 135 ± 20 mJ m^{-2} [30]. In [27], an experimental value of 75 mJ m^{-2} for γ_{TWB} is given.

We now discuss previous calculations. The results obtained by Vitek using an empirical pair potential for the interatomic interaction [31] are in good agreement with our first-principles results. He finds: 105, 95, and 55 mJ m^{-2} for the three fault energies. Recently, γ_{TWB} was calculated using a first-principles layer Korringa–Kohn–Rostoker method [32]. In that paper, the calculated γ_{TWB} of 118 mJ m^{-2} is considered to be in excellent agreement with an experimental result of 166 mJ m^{-2}. However, in a later paper [33] the result of 118 mJ m^{-2} was corrected to be the fault energy of the ESF. For γ_{ISF} and γ_{TWB} energies of 124 mJ m^{-2} and 56 mJ m^{-2}, respectively, are reported, in excellent agreement with our results. The quoted experimental result of 166 mJ m^{-2} is for the ISF [27]. Very recently, stacking fault energies for Al were obtained using the LMTO-ASA method and large supercells [34]. The results ($\gamma_{ISF} = 280 \pm 40$ mJ m^{-2}, $\gamma_{ESF} \simeq 260$ mJ m^{-2}, and $\gamma_{TWB} = 130 \pm 15$ mJ m^{-2}) are more than a factor of two larger than our results. Erroneously, good agreement with the value of 118 mJ m^{-2} for γ_{TWB} from [32] is claimed (see above). From the suggested reasons for the discrepancy between the LMTO-ASA results and experiment, the effect of the finite size of the supercell and/or of the neglect of interactions between the two faults is in our opinion the most likely one. In our approach, based on the connection with polytypes, the problem of finite supercells is to a large extent avoided.

We conclude this section by observing that we have succeeded in calculating from first-principles stacking-fault energies in Al with greater accuracy than they can be obtained from experiments up to now.

4. Point defects in aluminium

The vacancy and self-interstitial in Al are studied using N-atom supercells representing bulk Al ($N = 8, 16, 27$). For the vacancy we remove one atom from the cell, for the interstitial we add one atom at the (most symmetric) octahedral interstitial site, where it has six-fold coordination. Of course one can consider other sites for the interstitial atom as well, but the octahedral-site interstitial is expected to deform least the host crystal. Because the smallest deformations will lead to the largest possible choice for the muffin-tin radius R_{MT}, the chosen configuration for the interstitial allows for the most accurate calculation (see section 2). We note that both from experiment and theory it is known that *not* the octahedral interstitial, but the 100-split interstitial, or 'dumbbell', is the lowest-energy configuration [35]. The formation energies of both interstitial defect configurations are expected to be of similar magnitude. The removed (added) atom can be thought of to go to (come from) the surface of the crystal (see figure 2). We define the formation energies at constant volume of these point defects to be:

$$E_{f,v}^{vac} = E_{tot}(N-1;\Omega) - \frac{N-1}{N}E_{tot}(N;\Omega)$$
$$E_{f,v}^{int} = E_{tot}(N+1;\Omega) - \frac{N+1}{N}E_{tot}(N;\Omega) \qquad (4)$$

where $E_{tot}(N;\Omega)$ is the total energy of the N-atom cell with total volume Ω. Note that we do not contract (expand) the cell around the vacancy (interstitial) in order to obtain the same volume per atom in the $N-1$ ($N+1$) and N-atom cell (contrary to [10]). Adopting the latter approach would provide an equally valid definition of the (constant volume) formation energy, which becomes equivalent to our definition in the large-N limit. Our approach is expected to give less sensitivity of calculated results with respect to cell size, since the immediate vicinity of the defect is a better representation of that of the isolated defect, because the interatomic distances are not related to the cell size. We emphasize that we do include relaxations of the atoms around the defect.

Table 7. Vacancy formation energy at constant volume (in eV) as a function of cell size and Brillouin-zone sampling. The numbers of k points quoted from the scheme of [17] are for the full BZ of the respective supercells; in actual calculations they are reduced to a smaller number depending on the symmetry (perfect crystal or crystal with vacancy).

	Cell size		
N_{BZ}	8	16	27
8	0.62	0.98	0.98
64	0.93	0.76	—
216	0.83	—	—
512	0.83	—	—

4.1. The vacancy

For the vacancy we have calculated $E_{f,v}^{vac}$ using various cell sizes up to $N=27$ and various k point sets [17]. Results are presented in table 7. We also tested the dependence of $E_{f,v}^{vac}$ upon increasing the energy cut-off E_{PW}; for all three cell sizes $E_{f,v}^{vac}$ never changed by more than 0.005 eV by going from 6 to 8 Ryd. For the 8-atom cell all forces are zero by symmetry, so that the atoms around the vacancy cannot be relaxed. All calculations are fully converged regarding self-consistency and with respect to the number of plane waves. Only for the 8-atom cell are we able to fully converge the result with respect to increasing the number of k points. From calculations in both the 16- and 27-atom cell, we find that relaxation only lowers $E_{f,v}^{vac}$ by 0.10 eV. Our final result is therefore obtained as the converged result of the 8-atom cell corrected for relaxation: $E_{f,v}^{vac} = 0.73 \pm 0.10$ eV. This result agrees very well with the value 0.76 eV obtained in the 16-atom cell with our largest k point set, where we do include relaxation. Despite Friedel oscillations in the effective interaction between ions, which can be very long ranged in simple metals, it is not necessary to use larger supercells than we do. The total energy and therefore the vacancy formation energy can be insensitive to these oscillations. Our results as well as those of [11] indicate that the vacancy formation energy is indeed insensitive to the Friedel oscillations. This insensitivity can be understood from the work of Harrison and Wills [36], where it is shown that the effective interaction between ions in simple metals when used to compute total energies may be represented by a screened Coulomb form which decays exponentially. The agreement of our final result for $E_{f,v}^{vac}$ with the experimental result [37] of 0.66 ± 0.02 eV is very good, but these numbers may not be directly compared: experiment measures the formation *enthalpy* at constant *pressure*, ΔH_p, at a high temperature (about 600 K in [37]), whereas this quantity only equals the formation *energy* at constant *volume*, ΔU_v, for $T = 0$ (at which our calculation is valid). In [38], the following relation is derived for the formation of defects in general:

$$\Delta H_p = \Delta U_v - T\alpha_p \Omega \Delta P_v \tag{5}$$

where α_p is the linear expansion coefficient (at constant pressure), Ω the volume, and ΔP_v the change in pressure upon formation of the defect (at constant volume). Extrapolating either the experimental result to $T = 0$ or our calculated result to finite T (note that ΔU_v in general is temperature dependent [39]) is largely a matter of speculation and we will make no attempt here. Combining our method with molecular dynamics, enabling the introduction of temperature into the calculations, would open the way to a fully *ab initio* description of the thermodynamics of defects. Other recent studies find values for $E_{f,v}^{vac}$ ranging from 0.5 to 1.0 eV [10, 11, 20]. Our approach improves upon the latter studies in various aspects: in [11], a large dependence upon the choice of pseudopotential was found and no relaxation of the atoms around the vacancy was taken into account. In [10], a local pseudopotential was used, whereas an *ab initio* pseudopotential is non-local. The effect of the latter approximation remained to be investigated. In [20], computational limitations prevented a full study of the numerical approximations involved. In the present calculation, no pseudopotentials are used, all atomic relaxations are taken into account, and the effects of all numerical approximations are scrutinized.

With regard to relaxation around the vacancy, we find that the atoms closest to the vacancy move inward (the vacancy contracts) by 1.8% of the Al–Al distance in the bulk (d(Al–Al)). In contrast, a vacancy at a surface of Al expands because of

the tensile stress at the Al surface [40]. Although bonding in a semiconductor like Si is entirely different, the same phenomena occur: a vacancy in the bulk contracts (by about 3% of a bond length, lowering the energy by 0.1 eV), whereas one at the surface expands [41]. The formation energy of a vacancy in Si is much larger however: about 4.5 eV.

We have also calculated the migration energy at constant volume for the vacancy, $E^{vac}_{m,v}$. We have assumed that in the saddle-point configuration for the migration of a vacancy an Al atom is located halfway between the vacancy and the original position of this Al atom. The difference in energy between this configuration (after all the atoms have been allowed to relax in accordance with the calculated forces) and the relaxed vacancy then equals $E^{vac}_{m,v}$. We find: $E^{vac}_{m,v} = 0.7 \pm 0.2$ eV, in good agreement with the experimental result of 0.62 eV [42]. In the relaxed saddle-point configuration, the (four) neighbouring Al atoms have moved from their lattice positions by 5.7% of d(Al–Al), lowering the energy by 0.4 eV with respect to the unrelaxed saddle-point configuration [43].

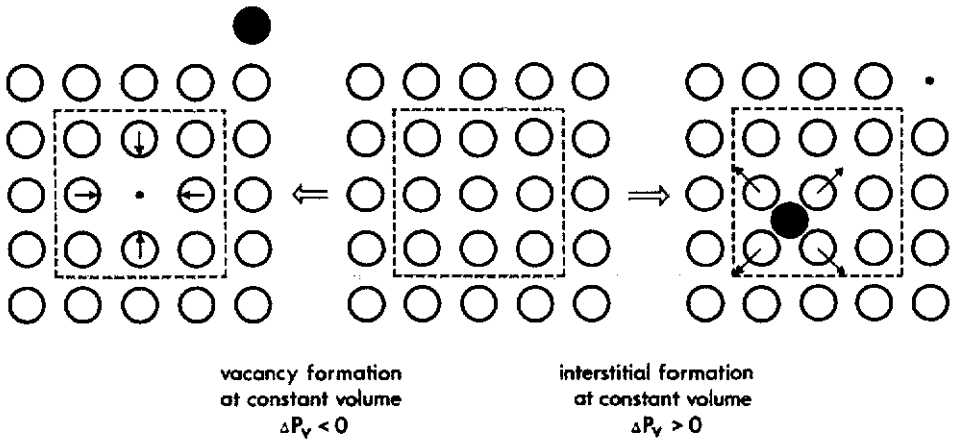

Figure 2. Schematic representation of the formation of point defects at constant volume. Vacancy formation proceeds by removing one atom from its lattice position and taking it to the surface of the crystal. The atoms surrounding the vacancy will move slightly towards the vacant site, but the total crystal volume is kept fixed. For self-interstitial formation, one atom is taken from the surface and brought to an interstitial site. The neighbouring atoms will move away from the interstitial by a substantial fraction of the nearest-neighbour distance in the perfect crystal, but the total crystal volume is again kept fixed. In calculations of the formation energy, the defective crystal is described using a supercell (represented by the dashed box) containing the defect, but not the surface. The extra or missing atom is accounted for by scaling the perfect-crystal result, in which all atoms are equivalent, by the appropriate factor (equation (4)).

Another interesting property of a defect is its formation volume at constant pressure, $\Delta\Omega_p$. For the vacancy we have: $\Delta\Omega_p = \Omega_0 + \Delta\Omega_{rel}$, where Ω_0 is the volume per bulk atom and $\Delta\Omega_{rel}$ is the change in volume upon relaxation of the lattice constant after the vacancy has been formed. The first term accounts for the atom that has gone to the surface upon vacancy formation (see figure 2). By carefully comparing the volume at which the total energy is a minimum for a supercell without and with the (relaxed) vacancy, we obtain $\Delta\Omega_{rel} = -0.35\Omega_0$. Therefore, $\Delta\Omega_p = 0.65\Omega_0$, again in very good agreement with the experimental value of $0.62\Omega_0$ [44]. We note that $\Delta\Omega_p$

is a very sensitive quantity to compute; for instance, if we would assume that the 16-atom supercell without vacancy has minimal energy for the same lattice constant as the (one-atom) primitive unit cell (using the same energy cut-off), we would find: $\Delta\Omega_p = 0.51\Omega_0$. In fact, the 16-atom cell has minimal energy for $a_c = 7.538$ au (cf $a_c = 7.56$ au for the primitive unit cell in section 2) and for the 15-atom cell (with one relaxed vacancy) the total energy is minimized for $a_c = 7.482$ au.

4.2. The octahedral-site self-interstitial

As has been argued in section 2, calculations for the self-interstitial defect are much more computing intensive. Moreover, relaxations of the six atoms around the interstitial at the octahedral site are much larger than for the vacancy, so that calculations in a $N = 8$ cell (in which we can converge the BZ integrations) are not expected to be very reliable. We succeeded in performing a calculation of $E_{f,v}^{int}$ in the $N = 16$ cell using the same k point sampling as in our best $N = 16$ calculation for the vacancy, which was reasonable converged with respect to enlarging the number of k points. Our results are compiled in table 8. Our best estimate for the interstitial is: $E_{f,v}^{int} = 3.4$ eV. The error bar on this result is estimated to be about 1 eV, but still the formation energy of this interstitial is a factor of about 5 larger than the formation energy of the vacancy. This result was to be expected on account of the fact that few experiments dealing with Al interstitials are known. We have provided the first quantitative estimate for $E_{f,v}^{int}$. Interstitials at other sites are expected to have larger formation energies (except for the 'dumbell'). If this expectation is indeed borne out, the vacancy is the only principal point defect to be reckoned with in studies of atomic diffusion in Al. A recent calculation [11] did not include relaxation of the atoms around the interstitial and found $E_{f,v}^{int} = 10$ eV. If in our calculation atomic relaxations are neglected we obtain: $E_{f,v}^{int} = 10.6$ eV, close to the result of [11]. As expected, relaxation is a big effect: an energy lowering of 7.2 eV and displacement of the atoms closest to the interstitial of 14% of d(Al–Al).

Table 8. Self-interstitial formation energy at constant volume (in eV) as a function of cell size and Brillouin-zone sampling. The numbers of k points quoted from the scheme of [17] are for the full BZ of the respective supercells; in actual calculations they are reduced to a smaller number depending on the symmetry (perfect crystal or crystal with interstitial).

	Cell size	
N_{BZ}	8	16
8	—	1.0
64	5.2	3.4

We also calculated the formation volume (at constant pressure), which for the interstitial is given by: $\Delta\Omega_p = -\Omega_0 + \Delta\Omega_{rel}$. The first term now accounts for the atom that has come from the surface, whereas the second term is the change in volume upon forming the defect (at constant pressure). As for the vacancy, the total energy is minimized in a supercell ($N = 16$) both without and with the interstitial present. In the case with the interstitial, the relaxation of the atoms around the interstitial is kept fixed (while changing the lattice constant) at the relaxation the atoms undergo for a volume corresponding to a lattice constant of 7.6 au The forces on the atoms

never deviate from zero appreciably for the lattice constants investigated. The cell without interstitial has minimal energy for $a_c = 7.630$ au and the cell with interstitial for $a_c = 7.854$ au, so that we have: $\Delta\Omega_p = 0.45\Omega_0$. The latter result should be considered with some caution. In the first place, the calculations in a 16-atom cell are for $N_{BZ} = 8$ (see table 8), which is probably not sufficient. Also the larger relaxation induced by the interstitial (compared to the vacancy) may necessitate a larger supercell. Taken together with the fact that $\Delta\Omega_p$ is a very sensitive quantity to compute (see above), we do not have a good estimate of its accuracy in this case. Moreover, one can derive the following relation [38]:

$$\Delta\Omega_p = -\Omega\kappa_T \Delta P_v \tag{6}$$

where Ω is the volume, κ_T the isothermal compressibility (which is the reciprocal of the bulk modulus B_0), and ΔP_v the change in pressure upon formation of the defect at constant volume. Since the energy is lowered by *increasing* the volume after putting in the interstitial, ΔP_v is positive (the pressure is positive after putting in the interstitial and zero before). Therefore, one would expect a negative $\Delta\Omega_p$. It is not inconceivable that our numerical approximations in this case render an accuracy consistent even with a negative $\Delta\Omega_p$, even though we find a rather large positive value. Note that the formation energy is calculated with better accuracy.

5. Conclusions

Using a new method for electronic structure calculations which besides total energy also gives the quantum mechanical forces on the atoms, we have calculated the energies and other properties of a wide variety of planar and point defects in the simple metal Al. Test calculations on ground state properties and phonons in bulk Al establish the reliability of the method. The results for defects, some of which have not (or not accurately) been extracted from experiment yet, may form a testing ground for effective interatomic potentials to be used in atomistic simulations of more complicated mechanical processes in metals. We have shown that on account of its much lower formation energy the vacancy is likely to be the more prominent point defect in Al. If our method is extended to include molecular dynamics simulation of the ionic degrees of freedom as well, the full (i.e., also $T \neq 0$) thermodynamics of defects can be studied, furthering our knowledge of the important effects of defects on material characteristics.

Acknowledgments

We acknowledge essential contributions of A R Williams in developing the methods used in this work. One of us (PJHD) thanks Alex Antonelli for useful correspondence. The computational work was carried out in the 'Electronic Structure of Materials' group at the University of Nijmegen. We further acknowledge financial support from the Foundation for Fundamental Research on Matter (FOM) (PJHD) and the Comision Interministerial de Ciencia y Tecnologia (CICyT) under project no PB86-0109 (JMS).

References

[1] Martin R M 1985 *Electronic Structure, Dynamics and Quantum Structural Properties of Condensed Matter* ed J T Devreese, P E van Camp (New York: Plenum)
Louie S G 1985 *Electronic Structure, Dynamics and Quantum Structural Properties of Condensed Matter* ed J T Devreese, P E van Camp (New York: Plenum)

[2] Tersoff J, Vanderbilt D and Vitek V (ed) 1989 *Atomic Scale Calculations in Materials Science (Materials Research Society Symp. Proc. 141)* (Pittsburgh, PA: MRS)

[3] Hellmann H 1937 *Einführung in der Quanten Theorie* (Leipzig: Deuticke) p 285
Feynman R P 1939 *Phys. Rev.* **56** 340

[4] Yin M T and Cohen M L 1982 *Phys. Rev.* B **26** 3259

[5] Denteneer P J H, Van de Walle C G and Pantelides S T 1990 *Phys. Rev.* B **41** 3885

[6] Car R and Parrinello M 1985 *Phys. Rev. Lett.* **55** 2471

[7] Soler J M and Williams A R 1989 *Phys. Rev.* B **40** 1560

[8] Andersen O K 1975 *Phys. Rev.* B **12** 3060

[9] Williams A R and Soler J M 1987 *Bull. Am. Phys. Soc.* **32** 562

[10] Gillan M J 1989 *J. Phys.: Condens. Matter* **1** 689

[11] Jansen R W and Klein B M 1989 *J. Phys.: Condens. Matter* **1** 8359

[12] Payne M C, Joannopoulos J D, Allan D C, Teter M P and Vanderbilt D H 1986 *Phys. Rev. Lett.* **56** 2656

[13] Soler J M and Williams A R 1990 *Phys. Rev.* B **42** 9728

[14] Soler J M and Williams A R 1991 to be published

[15] Denteneer P J H 1989 unpublished
The APW calculations are performed in a supercell geometry with 7 Si atoms, 1 H atom and a P atom originally at a substitutional site in the Si crystal.

[16] Denteneer P J H and Soler J M 1991 *Solid State Commun.* **78** 857

[17] Monkhorst H J and Pack J D 1976 *Phys. Rev.* B **13** 5188

[18] Fu C L and Ho K-M 1983 *Phys. Rev.* B **28** 5480

[19] The ground-state properties a_{eq} and B_0 are obtained from a fit of calculated total energies at five different lattice constants to Murnaghan's equation of state for solids (see e.g. [1]). In the APW calculations, 28 special points are used, and in the pseudopotential calculations 60 special points are used together with a kinetic energy cutoff of 24 Ryd (plane waves with energy between 12 and 24 Ryd are treated using Löwdin perturbation theory).

[20] See table 1 and references in Chakraborty B and Siegel R W 1983 *Phys. Rev.* B **27** 4535

[21] Hamann D R, Schlüter M and Chiang C 1979 *Phys. Rev. Lett.* **43** 1494

[22] Moruzzi V L, Janak J F and Williams A R 1978 *Calculated Electronic Properties of Metals* (New York: Pergamon)

[23] Lam P K and Cohen M L 1981 *Phys. Rev.* B **24** 4224; 1982 *Phys. Rev.* B **25** 6139

[24] Denteneer P J H and van Haeringen W 1987 *J. Phys. C: Solid State Phys.* **20** L883
Denteneer P J H in [2] p 343

[25] Smith J, Yeomans J and Heine V 1984 *Modulated Structure Materials* ed T Tsakalakos (Dordrecht: Martinus Nijhoff)

[26] Blandin A, Friedel J and Saada G 1966 *J. Physique Coll. Suppl.* 7–8 **27** C3 128

[27] Hirth J P and Lothe J 1982 *Theory of Dislocations* (New York: Wiley)

[28] Cheng C, Needs R J and Heine V 1988 *J. Phys. C: Solid State Phys.* **21** 1049

[29] MacDonald A H 1978 *Phys. Rev.* B **18** 5897

[30] Smallman R E and Dobson P S 1970 *Met. Trans.* **1** 2383

[31] Vitek V 1975 *Scr. Metall.* **9** 611

[32] MacLaren J M, Crampin S, Vvedensky D D and Eberhart M E 1989 *Phys. Rev. Lett.* **63** 2586

[33] Crampin S, Hampel K, Vvedensky D D and MacLaren J M 1990 *J. Mater. Res.* **5** 2107

[34] Xu J, Lin W and Freeman A J 1991 *Phys. Rev.* B **43** 2018

[35] Ehrhart P 1978 *J. Nucl. Mater.* **69/70** 200
Dederichs P H, Lehmann C, Schober H R, Scholz A and Zeller R 1978 *J. Nucl. Mater.* **69/70** 176

[36] Harrison W A and Wills J M 1982 *Phys. Rev.* B **25** 5007

[37] Fluss M J, Smedskjaer L C, Chason M K, Legnini D G and Siegel R W 1978 *Phys. Rev.* B **17** 3444

[38] Jacucci G and Taylor R 1979 *J. Phys. F: Met. Phys.* **9** 1489

[39] Jacucci G, Taylor R, Tenenbaum A and van Doan N 1981 *J. Phys. F: Met. Phys.* **11** 793

[40] Needs R J 1987 *Phys. Rev. Lett.* **58** 53
Feibelman P J 1989 *Phys. Rev. Lett.* **63** 2488

[41] Antonelli A and Bernholc J 1989 *Phys. Rev.* B **40** 10643
[42] Seeger A, Wolf D and Mehrer H 1971 *Phys. Stat. Solidi* b **48** 481
[43] The migration energy of the vacancy is calculated in a 16-atom cell using 64 **k** points in the BZ (see the caption of table 7).
[44] Emrick R M and McArdle P B 1969 *Phys. Rev.* **188** 1156